Journal of
Materials Chemistry A

Accepted Manuscript

This is an *Accepted Manuscript*, which has been through the RSC Publishing peer review process and has been accepted for publication.

Accepted Manuscripts are published online shortly after acceptance, which is prior to technical editing, formatting and proof reading. This free service from RSC Publishing allows authors to make their results available to the community, in citable form, before publication of the edited article. This *Accepted Manuscript* will be replaced by the edited and formatted *Advance Article* as soon as this is available.

To cite this manuscript please use its permanent Digital Object Identifier (DOI®), which is identical for all formats of publication.

More information about *Accepted Manuscripts* can be found in the **Information for Authors**.

Please note that technical editing may introduce minor changes to the text and/or graphics contained in the manuscript submitted by the author(s) which may alter content, and that the standard **Terms & Conditions** and the **ethical guidelines** that apply to the journal are still applicable. In no event shall the RSC be held responsible for any errors or omissions in these *Accepted Manuscript* manuscripts or any consequences arising from the use of any information contained in them.

Multi-walled carbon nanotube (MWCNT) attached pre-stitched graphene oxide (GO) was prepared and used as a reinforcing filler in linear low density polyethylene (LLDPE) composite. The tensile strength of the composite with 1 wt. % loading of the filler was enhanced dramatically by 148.7% compared to that of the neat LLDPE.

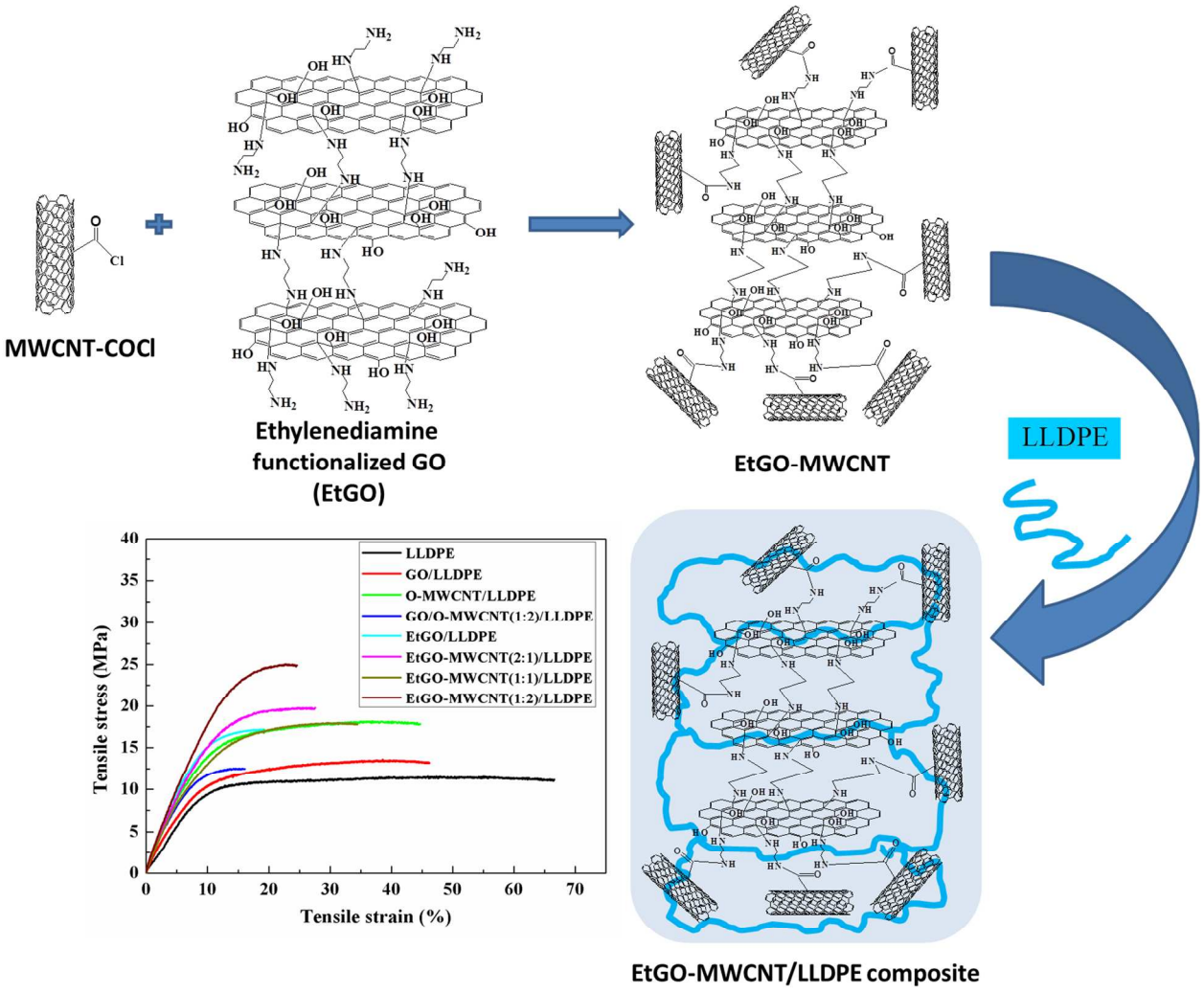

Journal of Materials Chemistry A

Cite this: DOI: 10.1039/c0xx00000x

www.rsc.org/xxxxxx

PAPER

Enhanced mechanical properties of multiwall carbon nanotube attached pre-stitched graphene oxide filled linear low density polyethylene composite

Nam Hoon Kim[a], Tapas Kuila[b], Joong Hee Lee[a,c,*]

A synergetic effect of multiwall carbon nanotube (MWCNT) attached pre-stitched graphene oxide (GO) on the mechanical properties of its linear low density polyethylene (LLDPE) composite was demonstrated. The reduction, functionalization and stitching of GO occurred simultaneously with the amine (-NH_2) functionalities of ethylenediamine through nucleophilic addition and condensation reaction. The structural features of MWCNT attached pre-stitched GO with ethylenediamine (EtGO) (EtGO-MWCNT) hybrids were confirmed by X-ray diffraction, Fourier transform infrared and Raman spectroscopy. EtGO-MWCNT hybrid filled LLDPE composite was prepared by solution mixing. The tensile strength of the EtGO-MWCNT/LLDPE composite with 1 wt.% loading was enhanced by 148.7 % compared to that of the neat LLDPE, which is the much higher than those of O-MWCNT, GO and EtGO filled composites. The enhanced properties of the EtGO-MWCNT/LLDPE composites were attributed to the homogeneous dispersion and the enhanced interfacial interaction with the matrix due to the multi-dimensional structure of EtGO-MWCNT. The EtGO-MWCNT/LLDPE composite also showed better dimensional stability than those of O-MWCNT, GO, and EtGO filled composites.

.

1. Introduction

Carbon nanostructures filled polymer composites find potential applications in thermal management, electronics, fuel cells, automobiles, transportation, etc. Different types of carbon-based nanofillers, such as carbon black, expanded graphite (EG), carbon nanotube (CNT), and carbon nanofiber (CNF) have been introduced to improve the mechanical, electrical and thermal properties of neat polymers. These carbon-based fillers have unique nanostructures, molecular level dispersion in the matrix polymer and superior properties as compared to bulk materials.[1-6] Among these carbon-based nanofillers, CNT has proven to be one of the successful fillers for polymer composites. However, it suffers from the limitations such as poor dispersion in polymeric matrices and high production cost as compared to other conventional fillers such as sodium montmorillonite, layered double hydroxide, exfoliated graphite, etc.[7-10]

The discovery of graphene in 2004 by Prof. A. K. Geim[11] has added a new era in science and engineering research. Graphene finds applications in the areas of field-effect transistors, drug delivery, hydrogen storage, polymer composites, biosensors, energy storage and conversion owing to its superior electrical, electrochemical, catalytic, thermal and mechanical properties.[12-15] Among these applications, the use of graphene or functionalized graphene as a reinforcing filler for polymer composites has been extensively studied for the fabrication of mechanically stable, thermally durable, and electrically conductive composite materials. The remarkable improvement in physicochemical properties of the composites is due to very large specific surface area, very high aspect ratio and outstanding mechanical flexibility of graphene. Therefore, graphene filled polymer composites have been regarded as promising materials for automotive component, aircrafts, nanoelectronics, transistors and supercapacitor devices.[16-20]

For the commercialization of graphene filled polymer composites, large scale production of graphene is required. It can be synthesized from naturally abundant and low cost graphite by a two-step oxidation-reduction approach. In this approach, first, graphite is oxidized to graphite oxide; a monolayer of graphene oxide (GO) is separated from multilayer graphite oxide; and then GO is reduced. However, the reduced GO (rGO) sheets often agglomerate to form a three-dimensional graphitic structure due to the van der Waals and π-π interaction. Moreover, the dispersion of rGO sheets in the organic polymer matrix is problematic due to the incompatible inorganic-organic surface contacts. Thus, surface modification of graphene is the best solution to prevent the agglomeration of individual rGO sheets and improve their dispersion in an organic polymer matrix.

Literature study showed that a very small amount of functionalized graphene or GO can enhance the mechanical, thermal, gas barrier, electrical and electrochemical performances of polymer composites compared to that of the neat polymer.[21-24] The improvements of physicochemical properties of the composites depend on the degree of dispersion of the filler, which again depend on the type of

surface modifier. It has been found that a long carbon chain surface modifier is effective for the improvement of mechanical properties, although thermal stability is lost due to the early degradation of the surface modifier. Long chain modifiers also decrease the electrical conductivity of the functionalized filler due to the insulating nature of the surface modifying agents. Thus, the use of short chain surface modifiers is encouraged for the simultaneous improvement of mechanical, thermal and electrical properties. However, insufficient surface compatible organic functionalities limit the degree of dispersion of the filler in the polymer matrix. Therefore, the optimization of graphene dispersion in the polymer matrix as well the reinforcing efficiency should be studied systematically. It has been found that the addition of a small amount of CNT along with graphene as a filler can improve the physicochemical properties of the composites owing to the synergistic effect of both fillers. However, these studies physically added two different kinds of fillers to the matrix to check their synergistic effects.[25-28]

Inspired by these studies, we can expect that multiwall carbon nanotube (MWCNT) attached pre-stitched GO can be used as effective reinforcing filler for the linear low density polyethylene (LLDPE). Herein, ethylenediamine is used to stitch GO sheets. This kind of stitching and surface modification can enhance the dispersion of the hybrid. Therefore, the present study aims to combine one dimensional MWCNT and two dimensional graphene to prepare a series of hybrid graphitic nanofillers and to observe the synergistic effect of the hybrid on the thermal, mechanical properties and dimensional stability of LLDPE-based composites.

2. Experimental

2.1. Materials

Natural graphite flakes were obtained from Sigma-Aldrich (Germany) and used as received. MWCNT (diameter 10-20 nm, length 10-50 μm) was purchased from Hanhwa Nanotech Co. Ltd., Korea. Sulfuric acid, hydrochloric acid, hydrogen peroxide and thionyl chloride were purchased from Samchun Pure Chemical Co. Ltd. (Korea). Potassium permanganate (Junsei Chemical Co. Ltd., Japan) was used as the oxidizing agent. Ethylenediamine (Sigma-Aldrich, Germany) were used for reduction and surface modification of GO. Anhydrous toluene (99.8 %) was purchased from Sigma-Aldrich and used as received. LLDPE (density, 944 kg m^{-3} at 23 °C) was supplied by Hanwha Chemical, Korea. 1,2-Dichlorobenzene (DCB) (Samchun Pure Chemical Co. Ltd, Korea) was used as the solvent to prepare the LLDPE composite.

2.2. Reduction and surface modification of GO

GO was prepared by the modified Hummer's method using natural graphite flakes.[29] The average thickness of as prepared GO was 0.9 nm, which was confirmed by the atomic force microscopic observation shown in Fig. S1 of the supporting information. The lateral dimension was in the range of 2-2.5 μm. The as-prepared material was suspended in DI-water containing dilute HCl solution to give a brown dispersion and washed repeatedly with DI-water to remove the acid and salts. The materials was then dispersed in water (0.5 mg ml^{-1}) by ultra-sonication (Sonosmasher ULH 700S, 20 kHz) to obtain a stable brown dispersion. The un-exfoliated graphite oxide was removed by centrifugation and a single layer of pure GO was used for further experimentation. In a typical experiment, ethylenediamine, $NH_2(CH_2)_2NH_2$ (600 mg), was dissolved in ethanol (35 ml) and added drop wise to a suspension of GO (200 mg) in water (33 ml) under vigorous stirring. The reaction continued for 24 h at room temperature. The resulting mixture was isolated by centrifugation, thoroughly washed with a 1:1 ethanol/water mixture and filtered by a dialysis tubing cellulose membrane (Sigma-Aldrich), followed by drying in a vacuum oven at 80 °C for 12 h prior to characterization.[30] The ethylenediamine functionalized graphene sheets were designated as EtGO.

2.3. Functionalization of MWCNT

The oxidation of MWCNT was performed with mixed acid (concentrated HNO_3 and H_2SO_4 taken in 1:3 ratio) at 110 °C for 1 h according to the procedure stated in the literature.[31] The oxidized MWCNT (O-MWCNT) was chlorinated using 100 mL of thionyl chloride ($SOCl_2$) at 70 °C for 24 h by stirring and reflux in N_2. The remaining $SOCl_2$ was removed by distillation and the resulting MWCNT-COCl powders were dried under vacuum at 70 °C for 24 h.[32]

2.4. Preparation of EtGO-MWCNT hybrid

The desired amounts of EtGO and MWCNT-COCl were first dispersed in 20 ml of anhydrous toluene (99.8 %, Sigma-Aldrich) by ultrasonication for 30 min and heated under N_2-purged reflux condition for 24 h at 70 °C with vigorous stirring. Finally, the hybrid EtGO and MWCNT powders washed repeatedly with a water-ethanol (1:1) mixture and dried under vacuum at 70 °C for 24 h.

2.5. Preparation of LLDPE composites

GO/LLDPE, O-MWCNT/LLDPE, GO/O-MWCNT/LLDPE, EtGO/LLDPE and EtGO-MWCNT/LLDPE composites were prepared by solution mixing. In brief, the desired amount of GO (1 wt.%) was dispersed in 40 ml of DCB by ultra-sonication at room temperature for 1 h. In a 250 ml Wit's apparatus, the desired amount of LLDPE was dissolved in 100 ml DCB at 140 °C to obtain a viscous solution. The dispersion of GO was then added to the polymer solution and stirred for 20 h at 140 °C. Finally, the composite solution was casted onto a Teflon Petri dish and dried at reduced pressure inside a vacuum oven at 75 °C to remove the solvent. O-MWCNT/LLDPE, GO/O-MWCNT/LLDPE, EtGO/LLDPE and EtGO-MWCNT/LLDPE composites were prepared with the same procedure. The dried composite materials were injection molded using HAAKE Minijet at 150 °C to obtain dumbbell shaped specimens for the tensile tests.

2.6. Characterization

Fourier transform infrared (FT-IR) spectra of the samples were recorded over a wave number range of 4000-400 cm^{-1} using a Nicolet 6700 spectrometer (Thermo Scientific, USA). X-ray diffraction (XRD) studies were carried out at room temperature on a X'pert Powder (PANalytical, Netherlands) at a scan rate of 2° min^{-1}. Raman spectra of EtGO-MWCNT were obtained on a Nanofinder 30 (Tokyo Instruments Co., Japan). The morphology of the EtGO-MWCNT hybrid and the fractured surface morphology of the entire composite surface were observed using Field emission scanning electron microscopy (FE-SEM), JSM-6701F (JEOL, Japan). The cryo-fracture surfaces of the composites were coated with a thin layer of platinum to improve the conductivity of the surfaces. Field emission transmission electron microscopy (FE-TEM) was carried out with a JEM-2200 FS (JEOL, Japan) at 200 kV to verify the morphology of EtGO-MWCNT hybrids in KBSI, Jeonju Center. Atomic force microscopy (AFM, XE-100, PARK System, South Korea) was used to observe GO with non-contact mode using a V-shaped 'ultralever' probe B. Thermogravimetric analysis (TGA) was also performed on a Q50 TGA (TA instruments, USA) at a heating rate of 5 °C min^{-1} from 50 to 700 °C in nitrogen. Tensile properties of neat LLDPE and its composites were measured on a universal testing machine, Landmark (MTS System Co., USA) according to the ASTM D-412 standard at a strain rate of 10 mm min^{-1} at 25 ± 2 °C. Dynamic mechanical analysis (DMA) of neat LLDPE and its composites were carried out with a Q 800 DMA (TA instruments, USA) in tension mode at a frequency and heating rate of 1 Hz and 2 °C min^{-1}. In order to measure the dimensional stabilities of neat LLDPE and its composites, thermomechanical analysis (TMA) were carried out with a Q 400 TMA (TA instruments, USA) at a heating rate of 3 °C min^{-1}.

3. Results and discussion

3.1 Proposed mechanism

As shown in Fig. 1(a), the carboxylic acid group on the edge of O-MWCNT can be converted to an acid chloride group by reaction with thionyl chloride. The surface of GO consists of different oxygen functional groups, such as epoxide, hydroxyl, and carboxyl groups. The $-NH_2$ functionalities of ethylenedimine molecules attack the epoxide carbon of GO and converts it into a hydroxyl group as shown in Fig. 1(b). The $-NH_2$ functionalities of ethylenedimine crosslink the GO sheets and form stitched graphene. After cross-linking of the GO sheets, the other end of the ethylenedimine remaining free ($-NH_2$ functional groups) is expected to directly couple with the -COCl functionalities of MWCNT, as shown in Fig. 1(c).

3.2 FT-IR spectra analysis

FT-IR spectra of GO, O-MWCNT and EtGO-MWCNT are shown in Fig. 2. Pure GO shows the characteristic peaks of -OH, -COOH, C-O-C (epoxy) at 3420, 1725 and 1224 cm^{-1}. A dramatic decrease in the intensities of the peaks corresponding to the presence of oxygen functionalities is observed after the reduction/stitching of GO sheets with ethylenediamine. The -COOH stretching vibration peak at 1725 cm^{-1} and the -OH deformation peaks (3420 and 1401 cm^{-1}) were decreased in the EtGO and EtGO-MWCNT hybrid. The intensities of the epoxy and alkoxy peaks at 1224 and 1057 cm^{-1} are also decreased in the EtGO-MWCNT hybrid with the ratios of 2:1 and 1:1. The disappearance or shrinkage of the oxygen functional groups in the EtGO and EtGO-MWCNT is attributed to their partial reductions by the amine functional groups of ethylenediamine, as indicated by earlier reports.[33-35] The appearance of new peaks at 1465 and 1260 cm^{-1} can be ascribed to the formation of strong in-plane C-N scissoring absorptions and C-O stretching vibrations. These kinds of bond formations can be explained by the nucleophilic substitution reaction of $-NH_2$ with the epoxide functionalities of GO. These findings not only confirm the removal of oxygen functionalities from the surface of GO, but also suggest nucleophilic additions and condensation reaction of ethylenediamine with GO sheets and -COCl activated MWCNT.

3.3 XRD analysis

XRD is used to ascertain the quality and crystallinity of a material. Fig. 3 shows the XRD patterns of GO, O-MWCNT, EtGO, and EtGO-MWCNT. Pristine graphite reveals a basal reflection (002) peak at 2θ = 26.6°corresponding to an interlayer distance of (d-spacing) of 0.34 nm.[36] However, after oxidation of pristine graphite, the 002 reflection peak of GO is shifted to 2θ =11.3° corresponding to an interlayer spacing of 0.77 nm. The increase in interlayer distance is due to the generation of oxygen functionalities in the basal plane of the graphite. It is also noted that the 002 reflection peak of O-MWCNT showed a downward shift at 2θ = 25.6° as compared to the raw MWCNT. This is attributed to the presence of oxygen functional groups between the two walls of the MWCNT, which can increase the interlayer spacing of the walls.[37] It is noteworthy that the 002 reflection peak has been shifted a lower angle (2θ = 9.8°) in EtGO as compared to pure GO. This may be attributed to the stitching of individual GO layers by the two amine functionalities present on the both sides of an ethylenediamine molecule. The less intense peak at 2θ = 26.5°of EtGO is also an indication of the stitching of GO sheets by ethylenediamine, although the formation of agglomerated reduced GO sheets cannot be ruled out.[30, 33] Interestingly, the 002 reflection peak of EtGO-MWCNT hybrid becomes prominent when the ratio of EtGO:MWCNT is 2:1. However, this peak of the EtGO-MWCNT hybrid almost disappears when the ratios are 1:1 and 1:2. It may be due to the main domain change of the hybrid fillers from GO to MWCNT, indicating that the hybrid fillers are uniformly dispersed and prevented from the agglomeration of rGO sheets as reported by Wang et al.[38]

3.4 Raman spectra analysis

Raman spectra were utilized to investigate the surface defects and the quality of the crystalline structure of the EtGO-MWCNT hybrid. Fig. 4 shows the Raman spectra of GO, EtGO, O-MWCNT and the EtGO-MWCNT hybrid. Graphitic materials can be identified by the appearance of a highly intense G band at 1575 cm^{-1} originated from the in-plane vibration of aromatic carbons and attributed to the doubly degenerate (E_{2g}) phonon mode symmetry. A comparatively low intense peak at 1345 cm^{-1} (D-band) is attributed to the k-point phonons of A_{1g} symmetry indicating the presence of defects as compared to the bulk graphite. The intensity of the D-band increases with increasing defect content in graphitic materials through oxidation, surface modification, vacancies, and doping of heteroatom in the sp^2 network. The appearances of D (1353 cm^{-1}) band at the lower region and the G band (1590 cm^{-1}) at higher region of GO is due to the extensive oxidation and the presence of sp^3 carbon environments. After reduction, the G-band of GO is shifted to 1574 cm^{-1} in EtGO illustrating the partial restoration of the π-electronic conjugated network. In contrast, the D-band appears at 1348 cm^{-1} and the intensity was increased suggesting successful functionalization and increased defect content in reduced GO. In addition, the intensity ratio of the D band to the G band is a measure of sp^3 surface defects within the sp^2 network structure of graphitic materials. It was noted that the intensity ratio of the D to G band (I_D/I_G) of GO (0.93) significantly decreased to 0.89 after treatment with ethylenediamine. The increased I_D/I_G ratio of the hybrid material containing higher amount of O-MWCNT suggests the presence of sp^3 defects due to the homogeneous intercalation of O-MWCNT between graphene sheets.

3.5 Mechanical properties

Fig. 5 shows the stress-strain curves of neat LLDPE and GO, O-MWCNT, GO/O-MWCNT, EtGO and EtGO-MWCNT filled LLDPE composites (1 wt.% fillers). The tensile strength, modulus, and elongation at break are summarized in Table 1. The composites filled with GO, O-MWCNT, GO/O-MWCNT, EtGO and EtGO-MWCNT show improved tensile behavior compared to the neat LLDPE. Interestingly, the O-MWCNT filled composite shows higher tensile strength than those of GO and EtGO filled composites. This is due to the better dispersion of O-MWCNT in the LLDPE matrix and higher aspect ratios of O-MWCNT than that of GO and EtGO. The addition of EtGO-MWCNT (1:2) significantly increased the tensile strength (23.2 MPa) and modulus (1.55 GPa) of the LLDPE composite, which implied 107 and 131 % improvement as compared to the neat LLDPE. However, the elongation at break was decreased remarkably due to the restricted movement of the matrix with the addition of the multidimensional filler, which allowed better matrix-filler interaction than single filler.[25,39] It is noteworthy that the composite filled with the un-stitched hybrid filler (GO/O-MWCNT) reveals that the tensile strength and elongation at break are significantly lower than those of the composites filled with stitched hybrid filler or O-MWCNT. It was attributed to the inferior dispersion of unstitched hybrid in the LLDPE matrix and the weak interaction between fillers and matrix. This observation confirms that the stitching of EtGO and O-MWCNT plays an important role in the improvement of mechanical properties of the composites.

3.6 FE-SEM and TEM analysis

The FE-SEM images show the surface morphology of the EtGO-MWCNT hybrid filler, which is remarkably different from those of carbon black, CNT, and graphite, as shown in Fig. 6. The images clearly show the homogeneous dispersion of MWCNTs with the graphene sheets. The distribution of MWCNT remained homogeneous even at higher loadings. The TEM images of the hybrid filler for different weight ratios (2:1, 1:1 and 1:2) of EtGO and MWCNT are shown in Fig. 7. The MWCNT were entangled into bundles and homogeneously distributed on the graphene sheets. The small pieces of graphene-like sheets were attached to the MWCNT bundles. The distribution of MWCNT on the EtGO sheets remained homogeneous even after increasing the content of MWCNT (Fig. 7(e)). The selected area electron diffraction (SAED) pattern of the hybrid filler (EtGO-MWCNT (2:1)) consists of many diffraction spots, suggesting the destroyed long-range ordering between the EtGO sheets.

The cryo-fractured specimens of various LLDPE-based composites were observed through FE-SEM to correlate the mechanical properties of the composites with morphologies (Fig. 8). Examination of the FE-SEM images of the neat LLDPE and composite samples revealed their significant difference in fractured surfaces. The fractured surfaces of the neat LLDPE were smooth, plain and glassy, confirming the failure of this material occurred at low stress. In contrast, the fractured surfaces of the composites with the EtGO-MWCNT hybrid filler became rough, indicating improved mechanical properties. The surface of the composite with EtGO-MWCNT (1:2) became the roughest among the samples. The formation of rough fracture surfaces is attributed to the multi-dimensional structure of the stitched hybrid filler and the comparatively soft polymer chain of the stitching segment, which enhance load transfer from the matrix to the hybrid filler. In contrast to the previously reported work with MWCNT,[40] it is hard to observe the pulled out fibers even in the rough fracture surfaces.

3.7 TGA

Thermal stabilities of pure GO and different EtGO-MWCNT hybrids are shown in Fig. 9. The thermal stabilities of the hybrid materials increase with increasing MWCNT content. This is attributed to the presence of labile oxygen functionalities on the surface of GO. Moreover, the ethylenediamine molecules plays an important roles in removing the oxygen functionalities from the surfaces of GO and oxidized MWCNT. This kind of oxygen functional groups removal from the surface of GO or O-MWCNT enhances the thermal stability of the hybrid filler. Interestingly, the thermal stability of the EtGO-MWCNT hybrid filler of EtGO-MWCNT (1:2) is comparatively higher than those of the EtGO-MWCNT (2:1) and EtGO-MWCNT (1:1).

Thermal stability of neat LLDPE as well as its composites with different fillers was investigated by TGA, as shown in Fig. 10. The TG profile shown in Fig. 10 reveals that the hybrid fillers are effective in terms of enhancing the thermal stability of the composites. It can be easily seen in the enlarged inset. The degradation temperature at 5 % weight loss for neat LLDPE was 379 °C. In contrast, the thermal stability was improved significantly with the additions of GO, O-MWCNT, EtGO, and EGO-MWCNT hybrid fillers.

The degradation temperature at 5 % weight loss of the composites with EGO-MWCNT (1:2) was enhanced to 407 °C. Similarly, the thermal stabilities of the composites up to 40 % weight loss always remained higher than that of the neat LLDPE. The enhanced thermal stabilities of the composites were due to the very high aspect ratios of GO and MWCNT, which prevented the emission of thermally degraded small gaseous molecules. The homogeneous dispersion of GO, MWCNT and the hybrid filler can also act as barrier to disrupt the oxygen supply from the atmosphere to the bulk of the sample during degradation/burning. Interestingly, the composite with the EtGO-MWCNT (1:2) hybrid filler showed highest thermal stability. The improved efficiency of the hybrid filler as compared to the individual fillers can be ascribed due to the synergistic effect of GO and MWCNT, which causes good matrix-filler interaction. This observation is in good agreement with the observation of the mechanical properties of the composites, further confirming the optimal reinforcing efficiency of the hybrid filler.

3.8 DMA analysis

The storage modulus (E') of neat LLDPE and GO, O-MWCNT, EtGO and EtGO-MWCNT composites are shown in Fig. 11(a). The storage modulus of the composites was measured in the temperature range of -90 to 100 °C. The storage modulus of the composites is always higher than that of the neat LLDPE and is found to be superior for the composites containing hybrid filler. This is due to the better reinforcing effect of the hybrid filler than pure GO, O-MWCNT and EtGO (1 wt.% loadings) fillers. The EtGO-MWCNT hybrid structures play an important role in the dispersion and reinforcing effect of fillers. The storage modulus of the EtGO-MWCNT (1:2) filled composite at -70 °C is 155 % higher than that of the neat LLDPE. In contrast, the storage modulus of the EtGO-MWCNT composites with EtGO-MWCNT ratios of 2:1 and 1:1 increased by 149 and 130 %, respectively. Interestingly, the storage modulus of the EtGO-MWCNT (1:2) filled composites at 50 °C was almost similar (157 %) to that of the neat LLDPE.

The effect of the hybrid filler on the tan δ values of its composites are shown in Fig. 11(b). The α-relaxation peak of neat LLDPE and its composites appeared in the temperature range of -30 to -25 °C. In contrast, the β- relaxation peak appeared at 80-90 °C. These observations are in good agreement with the observation of Kuila et al. for functionalized graphene/LLDPE composites.[41] In their study, the peak values of the tan were significantly lower than that of the neat LLDPE. This is attributed to the reinforcing and synergistic effect of the hybrid filler, which decreased the damping behavior of the composites.

3.9 TMA analysis

The variations of the dimensional stabilities of neat LLDPE and its composites according to the type and content of the filler (GO, O-MWCNT, EtGO, and EtGO-MWCNT) and temperature are shown in Fig. 12(a). The slope of the graph for the EtGO-MWCNT/LLDPE composites was much lower than those of the neat LLDPE and the composites containing single fillers (GO or EtGO or O-MWCNT). This is due to the homogeneous dispersion and synergistic effect of the hybrid filler in the matrix and increased hardness proportional to the filler content.[37] The change in dimensional stability was very small in the composites with the EtGO-MWCNT hybrid fillers.

The coefficients of thermal expansion (CTE) values of the various composites were calculated over 40-100 °C from the TMA curves and are shown in Fig. 12(b). The CTE value of the LLDPE was not significantly changed by the addition of GO, but it decreased remarkably with the addition of the stitched hybrid filler (EtGO-MWCNT). This decreased CTE value of the EtGO-MWCNT/LLDPE composite is attributed to the homogeneous dispersion of the fillers in the matrix and strong interactions between fillers and matrix due to the multi-dimensional structure of the hybrid filler and chemical functionalities on the surface of the filler.[42]

4. Conclusions

We successfully prepared a hybrid filler using GO and O-MWCNT. Ethylenediamine was used to cross-link GO and O-MWCNT. In addition, the ethylenediamine molecules acted as a reducing, cross-linking and functionalizing agent at the same time. The structural features of the hybrid material were confirmed by XRD, FTIR and Raman spectroscopy. The thermal stabilities of EtGO-MWCNT hybrid was examined by TGA. The dispersion of MWCNT in graphene was determined by FE-SEM and TEM analysis. The as-prepared hybrid filler was used to prepare its LLDPE-based composite by solution mixing. The LLDPE-based composite materials exhibited enhanced mechanical properties as compared to neat LLDPE because of the homogenous dispersion of the hybrid filler and the synergistic effect of graphene and MWCNT. It is seen that the improvement in tensile strength at break for the EtGO-MWCNT (1:2) filled LLDPE composites was significantly higher than that of the other composites. In contrast, the elongation at break for the EtGO-MWCNT (1:2) filled LLDPE composites has been found to be lowest among the studied system. The increase in tensile strength and decrease in elongation at break is the indication for the formation of stiffened composites. This observation is well supported by the dynamic mechanical analysis. It showed that EtGO-MWCNT filled composites are equally useful both at cryogenic and ambient conditions. The improvement in mechanical properties of the composites was in-line with the observation of tensile fracture surface analysis. Thermal

stabilities of the composites were also improved as evidenced by TGA. Therefore, it is seen that the simultaneous reduction, functionalization and stitching of GO and -COCl activated MWCNT using ethylenediamine as a cross-linking agent could be a promising hybrid filler to fabricate graphene based polymer composites with effective reinforced performance.

Acknowledgements

This study was supported by the Converging Research Center Program (2013K000404) through the Ministry of Science, ICT & Future Planning and the Basic Science Research Program through the National Research Foundation (NRF) funded by the Ministry of Education of Korea (NRF-2013R1A1A2011608). It was also supported by research funds of Chonbuk National University in 2013.

Notes and references

[a]Advanced Materials Research Institute for BIN Fusion Technology (BK Plus Global Program), Department of BIN Fusion Technology, Chonbuk National University, Jeonju, Jeonbuk, 561-756, Republic of Korea.

[b]Surface Engineering & Tribology Division, CSIR-Central Mechanical Engineering Research Institute, Council of Scientific & Industrial Research (CSIR), Mahatma Gandhi Avenue, Durgapur-713209, India.

[c]Advanced Wind Power System Research Center, Department of Polymer & Nano Engineering, Chonbuk National University, Jeonju, Jeonbuk, 561-756, Republic of Korea. Fax: +82 63 2702341; Tel: +82 63 270 2342

*Correspondence to: jhl@jbnu.ac.kr

1. Z. Spitalsky, D. Tasis, K. Papagelis and C. Galiotis, *Prog. Polym. Sci.*, 2010, **35**, 357-401.
2. Y. C. Li and G. H. Chen, *Polym. Eng. Sci*., 2007, **47**, 882-888.
3. A. Yasmin, J. J. Luo and I. M. Daniel, *Compos. Sci. Technol*., 2006, **66**, 1182-1189.
4. T. Jeevananda, Y. K. Jang, J. H. Lee, B. Siddaramaiah, M. V. Deepa Urs and C. Ranganathaiah, *Polym. Int.,* 2009, **58**, 755-780.
5. A. Yu, P. Ramesh, M. E. Itkis, B. Elena and R. C. Haddon, *J. Phys. Chem. C.,* 2007, **111**, 7565-7569.
6. G. G. Tibbetts, M. L. Lake, K. L. Strong and B. P. Rice, *Compos. Sci. Technol.*, 2007, **67**, 1709-1718.
7. M. Alexandre and P. Dubois, *Mater. Sci. Eng:R*, 2000, **28**, 1-63.
8. S. S. Ray and M. Okamoto, *Prog. Polym. Sci.*, 2003, **28**, 1539-1641.
9. F. Leroux and J. P. Besse, *Chem. Mater.*, 2001, **13**, 3507-3515.
10. B. Debelak and K. Lafdi, *Carbon*, 2007, **45**, 1727-1734.
11. K. S. Novoselov, A. K. Geim, S. V. Morozov, D. Jiang, Y. Zhang, S. V. Dubonos, I. V. Grigorieva and A. A. Firsov, *Science,* 2004, **306**, 666-669.
12. S. Rosenblatt, Y. Yaish, J. W. Park, J. Gore, V. Sazonova and P. L. Mceuen, *Nano. Lett.,* 2002, **2**, 869-872.
13. A. Bianco, K. Kostarelos and M. Prato, *Curr. Opin. Chem. Biol.*, 2005, **9**, 674679.
14. C. Liu, Y. Chen, C. Z. Wu, S. T. Xu and H. M. Cheng, *Carbon*, 2010, **48**, 452-455.
15. R. H. Baughman, A. A. Zakhidov and W. A. de Heer. *Science*, 2002, **297**, 787-792.
16. R. Sengupta, M. Bhattacharya, S. Bandyopadhyay and A. K. Bhowmick, *Prog. Polym. Sci.*, 2011, **36**, 638-670.
17. X. Li, X. Wang, L. Zhang, S. Lee and H. Dai, *Science*, 2008, **319**, 1229-1231.
18. P. Blake, P. D. Brimicombe, R. R. Nair, T. J. Booth, D. Jiang, F. Schedin, L. A. Ponomarenko, S .V. Morozov, H. F. Gleeson, E. W. Hill, A. K. Geim and K. S. Novoselov, *Nano. Lett.,* 2008, **8**, 1704-1708.
19. H. Wang, Q. Hao, X. Yang, L. Lu and X. Wang, *Electrochem. Commun.*, 2009, **11**, 1158-1161.
20. S. Bose, T. Kuila, A. K. Mishra, R. Rajasekar, N. H. Kim and J. H. Lee. *J. Mater. Chem.*, 2012, **22**, 767-784.
21. S. Stankovich, D. A. Dikin, G. H. B. Dommett, K. M. Kohlhaas, E. J. Zimney, E. A. Stach, R. D. Piner, S. T. Nguyen and R. S. Ruoff, *Nature*, 2006, **442**, 282-286.
22. T. Kuila, S. Bhadra, D. Yao, N. H. Kim, S. Bose and J. H. Lee, *Prog. Polym. Sci.*, 2010, **35**, 1350-1375.
23. H. Liu, T. Kuila, N. H. Kim, B .C. Ku and J. H. Lee, *J. Mater. Chem. A.*, 2013, **1**, 3739-3746.
24. T. Kuila, S. Bose, C. E. Hong, M. E. Uddin, P. Khanra, N. H. Kim and J. H. Lee, *Carbon,* 2011, **49**, 1033-1037.
25. S. Y. Yang, W. N. Lin, Y. L. Huang, H. W. Tien, J. Y. Wang, C. C. M. Ma, S. M. Li and Y. S. Wang, *Carbon*, 2011, **49**, 793-803.
26. J. Li, P. S. Wong and J. K. Kim. *Mater. Sci. and Eng. A-Struct.,* 2008, **483**, 660-663.
27. B. P. Vinayan, R. Nagar, V. Raman, N. Rajalakshmi, K. S. Dhathathreyan and S. Ramaprabhu, *J. Mater. Chem.*, 2012, **22**, 9949-9956.
28. Q. Cheng, J. Tang, J. Ma, H. Zhang, N. Shinya, and L. C. Qin. *Phys. Chem. Chem. Phys.*, 2011, **13**, 17615-17624.
29. W. S. Hummers and R.E. Offeman, *J. Am. Chem. Soc.*, 1958, **80**, 1339.
30. H. A. Margarita, A. A. Ahmed, J. M. Michael, A. A. Ilhan and K.P. Robert, *Langmuir*, 2007, **23**, 10644-10649.
31. C. E. Hong, J. H. Lee, K. Prashantha and S. G. Advani, *Compos. Sci. Technol.*, 2007, **67**, 1027-1034.
32. J. S. Park, S. M. Cho, W. J. Kim, J. Park and P. J. Yoo, *ACS Appl. Mater. Interfaces.,* 2011, **3**, 360-368.
33. N. H. Kim, T. Kuila and J. H. Lee. *J. Mater. Chem. A.*, 2013, **1**, 1349-1358.
34. A. B. Bourlinos, D. Gournis, D. Petridis, T. Szabo´, A. Szeri and I. De´ka´ny, *Langmuir*, 2003, **19**, 6050-6055.
35. W. Li, X. Z. Tang, H. B. Zhang, Z. G. Jiang, Z. Z. Yu, X. S. Du and Y.W. Mai, *Carbon*, 2011, **49**, 4724-4730.
36. R. Bissessur, P. K.Y. Liu and S.F. Scully. *Synth. Met.*, 2006, **156**, 1023-1027.
37. H. B. Zhang, G. D. Lin, Z. H. Zhou, X. Dong and T. Chen, *Carbon*, 2002, **40**, 2429-2436.

38. Y. Wang, Y. Wu, Y. Huang, F. Zhang, X. Yang, Y. Ma and Y. Chen, *J. Phys. Chem. C.*, 2011, **115**, 23192-23197.
39. A. Yu, P. Ramesh, X. Sun, E. Bekyarova, M. E. Itkis and R. C. Haddon, *Adv. Mater.*, 2008, **20**, 4740-4744.
40. G. Yamamoto, K. Shirasu, T. Hashida, T. Takagi, J. W. Suk, J. An, R. D. Piner and R. S. Ruoff, *Carbon*, 2011, **49**, 3709-3716.
41. T. Kuila, S. Bose, A. K. Mishra, P. Khanra, N. H. Kim and J. H. Lee, *Polym. Test.*, 2012, **31**, 31-38.
42. L. M. Zhang and G. C. Dai, *Express Polym. Lett.,* 2007, **1**, 608-615.

Table 1. Tensile properties of neat LLDPE and GO, O-MWCNT, GO/O-MWCNT, EtGO and EtGO-MWCNT filled LLDPE composites (1 wt.%)

Sample	Tensile Strength (MPa)	Young's Modulus (GPa)	Elongation at break (%)
LLDPE	11.2	0.67	66.2
GO	13.6	0.78	46.1
O-MWCNT	17.8	1.00	44.5
GO/O-MWCNT (1:2)	12.5	1.50	16.0
EtGO	17.2	1.16	19.1
EtGO-MWCNT (2:1)	19.8	1.20	27.2
EtGO-MWCNT (1:1)	17.4	0.92	33.4
EtGO-MWCNT (1:2)	23.2	1.55	24.9

Figure Captions

Fig. 1 Schematic for the proposed mechanism of formations of (a) surface modified O-MWCNT, (b) EtGO, and (c) EtGO-MWCNT hybrid.

Fig. 2 FT-IR spectra of (a) GO, (b) O-MWCNT, (c) EtGO, (d) EtGO-MWCNT (2:1), (e) EtGO-MWCNT (1:1), and (f) EtGO-MWCNT (1:2).

Fig. 3 XRD patterns of (a) GO, (b) O-MWCNT, (c) EtGO, (d) EtGO-MWCNT (2:1), (e) EtGO-MWCNT (1:1), and (f) EtGO-MWCNT (1:2).

Fig. 4 Raman spectra of (a) GO, (b) O-MWCNT, (c) EtGO, (d) EtGO-MWCNT (2:1), (e) EtGO-MWCNT (1:1), and (f) EtGO-MWCNT (1:2).

Fig. 5 Stress-strain curves of neat LLDPE and its composites with various fillers (1 wt.%).

Fig. 6 FE-SEM images of the surfaces of (a,b) EtGO-MWCNT (2:1), (c,d) EtGO-MWCNT (1:1), and (e,f) EtGO-MWCNT (1:2).

Fig. 7 TEM, HR-TEM and SAED pattern images of (a, b) EtGO-MWCNT (2:1), (c,d) EtGO-MWCNT (1:1) and (e ,f) EtGO-MWCNT (1:2).

Fig. 8 FE-SEM images of the fractured surfaces of (a) neat LLDPE and LLDPE composites with (b) GO, (c) O-MWCNT, (d) EtGO-MWCNT (2:1), (e) EtGO-MWCNT (1:1), and (f) EtGO-MWCNT (1:2).

Fig. 9 TGA curves of pure GO, O-MWCNT, EtGO and EtGO-MWCNT.

Fig. 10 TGA curves of neat LLDPE and its composites with various fillers.

Fig. 11 Variations of (a) storage modulus and (b) tan δ values of neat LLDPE and GO, O-MWCNT, and EtGO-MWCNT filled LLDPE composites.

Fig. 12 (a) Variations of dimensional stabilities of neat LLDPE and its composites with temperature, (b) the coefficients of thermal expansion (CTE) of neat LLDPE and its composites in the range of 40-100 °C.

Figures

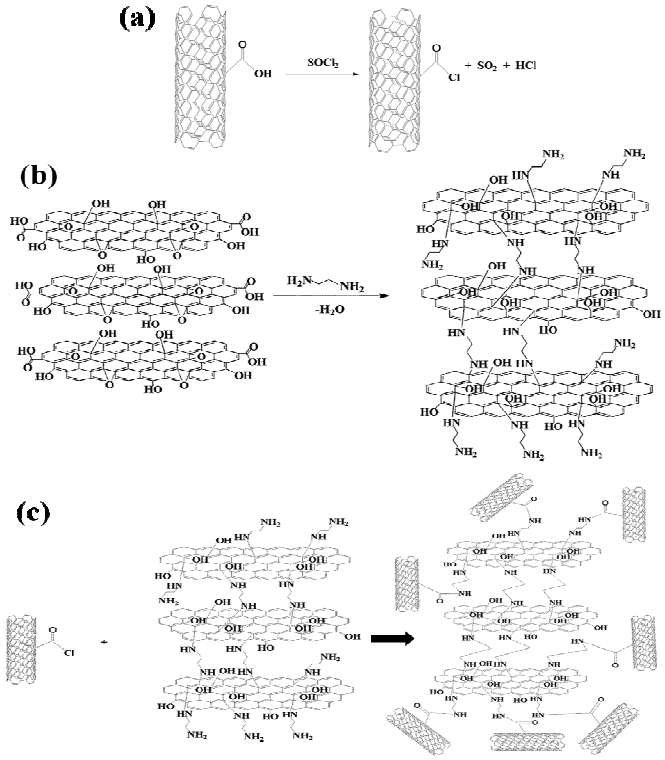

Fig. 1

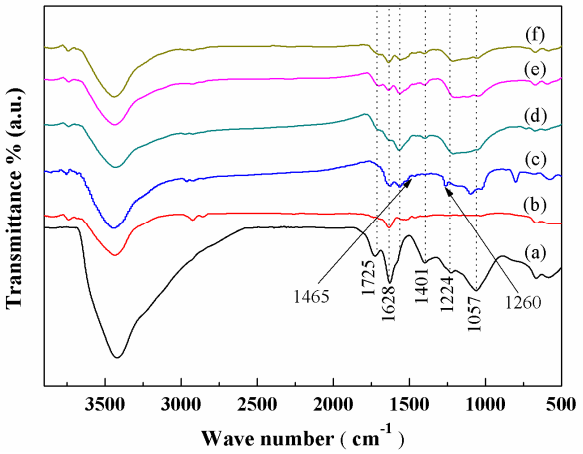

Fig. 2

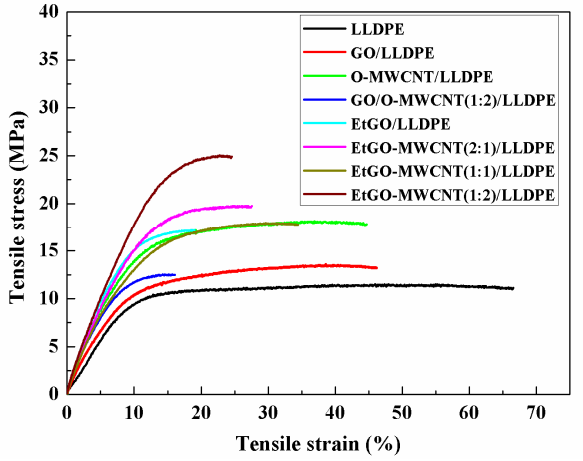

Fig.5

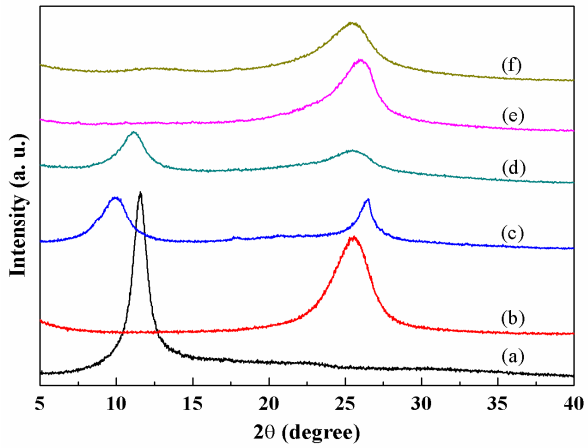

Fig. 3

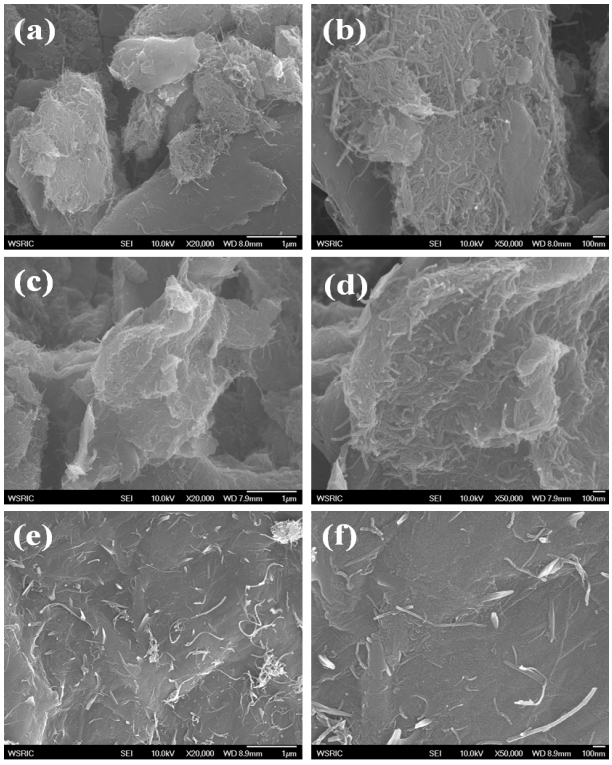

Fig. 6

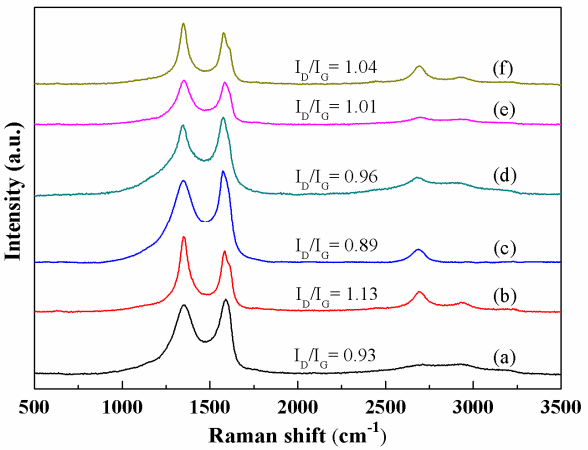

Fig.4

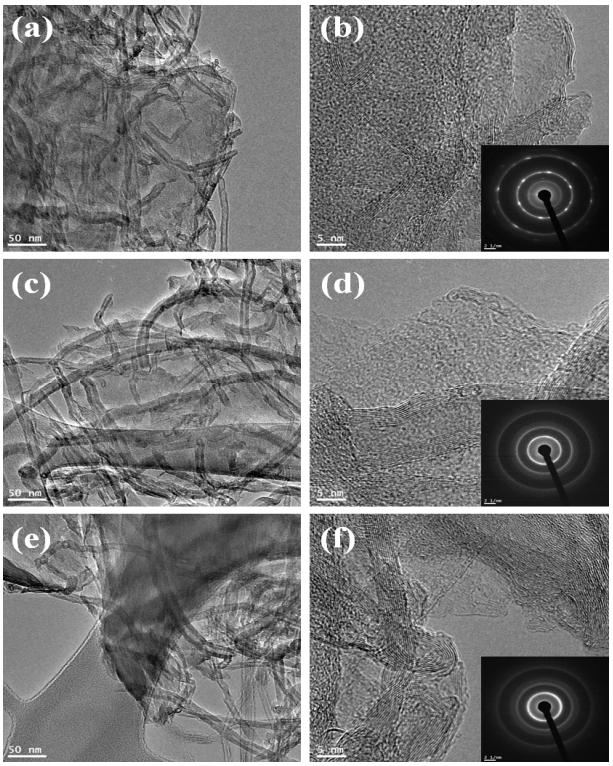

Fig. 7

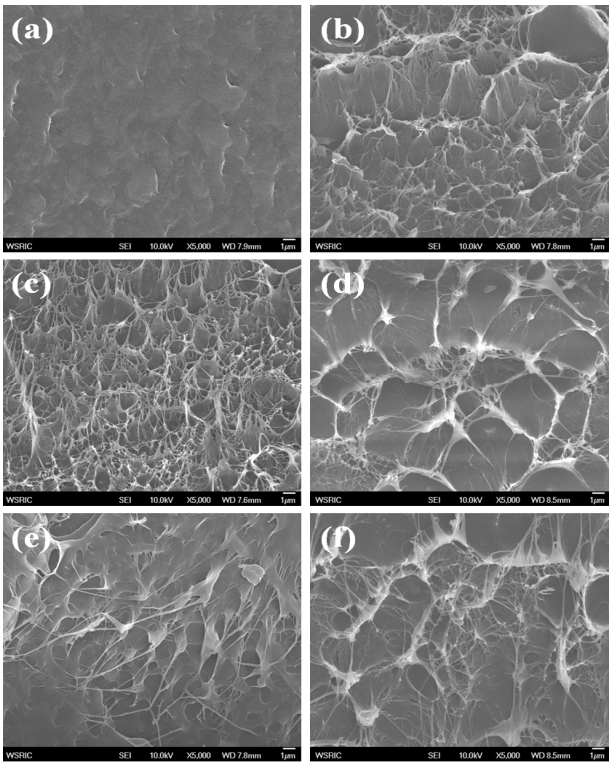

Fig.8

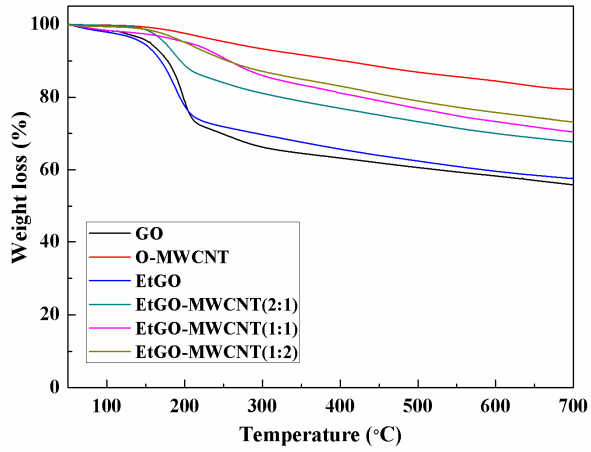

Fig.9

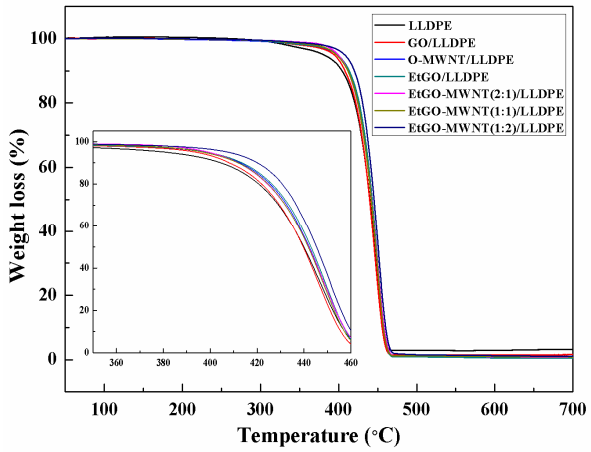

Fig.10

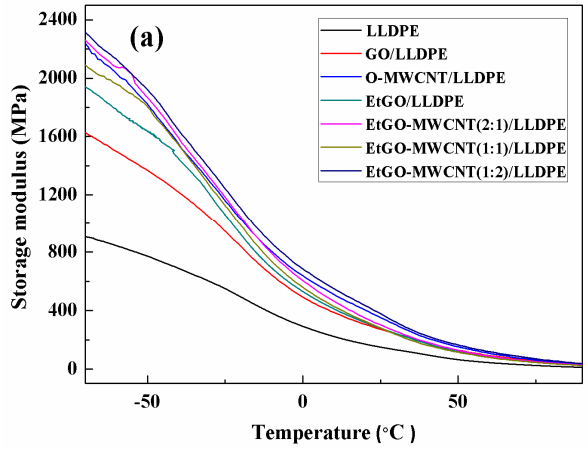

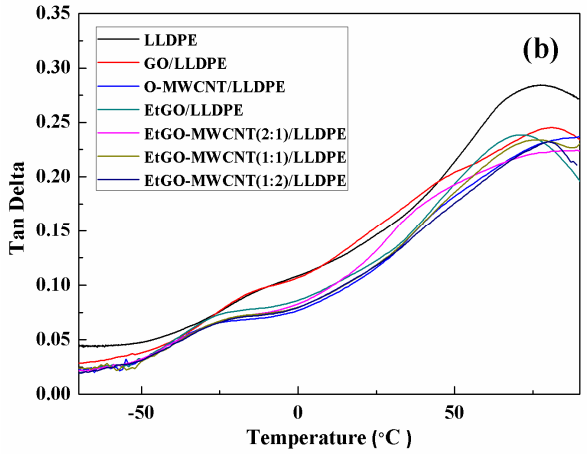

Fig.11

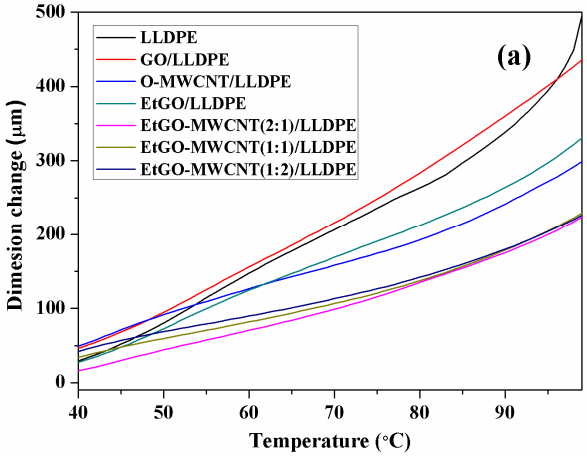

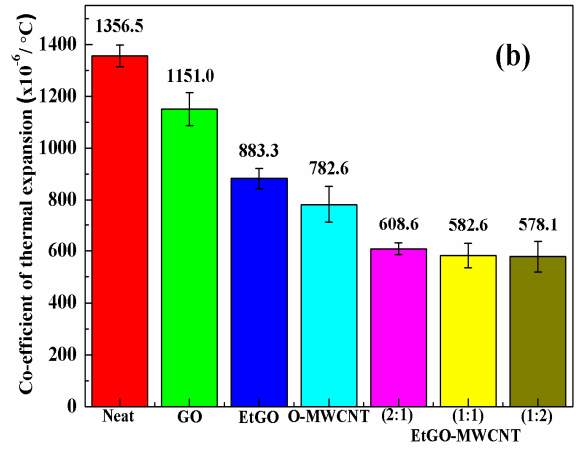

Fig.12

Table of Contents

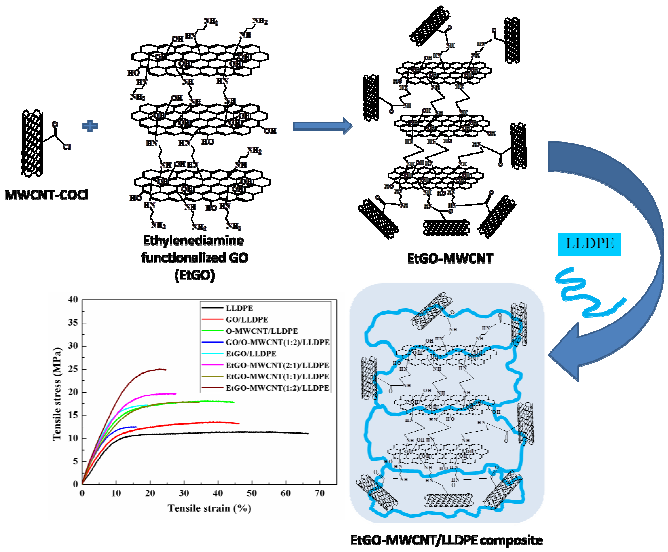

Multi-walled carbon nanotube (MWCNT) attached pre-stitched graphene oxide (GO) was prepared and used as a reinforcing filler in linear low density polyethylene (LLDPE) composite. The tensile strength of the composite with 1 wt. % loading of the filler was enhanced dramatically by 148.7% compared to that of the neat LLDPE.